Pergamon

Int. J. Heat Mass Transfer. Vol. 40, No. 5, pp. 1045–1051, 1997

0017–9310/97 $17.00 + 0.00

PII: S0017-9310(96)00214-1

Fin efficiency enhancement using a gravity-assisted planar heat pipe

JIE WEI,† KUNIO HIJIKATA and TAKAYOSHI INOUE

Department of Mechano-Aerospace Engineering, Tokyo Institute of Technology, 2-12-1 Ohokayama Meguro-ku, Tokyo, Japan

(*Received* 9 *November* 1995 *and in final form* 3 *May* 1996)

Abstract—An experimental and analytical study was conducted to evaluate a planar heat pipe used as a cooling fin for high density heat dissipation. Both natural and forced convection configurations were investigated. For forced convection, the thermal resistance of the heat pipe, 100 mm × 90 mm × 5 mm in dimensions, was more than three times smaller than that for a solid fin with the same dimensions when the heat dissipation rate exceeded 10 W cm^{-2} and the heating temperature was under 100°C. The improved performance makes planar heat pipes viable alternatives to conventional solid fins, for applications requiring efficient and reliable heat dissipation. Copyright © 1996 Elsevier Science Ltd.

INTRODUCTION

Applications involving performance reliability of high-power equipment, such as electromechanical and electronic equipment, depend strongly on the ability to maintain operating temperatures within acceptable limits. In air, natural convection fins are the most commonly used technique for enhancing heat dissipation because of their inherent reliability, simplicity and maintenance-free manner, and they are more reliable and versatile than forced convection fins. Since the heat dissipation rate in natural convection, less than 0.1 W cm^{-2} for allowable maximum temperature of 100°C, is extremely limited by the lower convection coefficient, large dimensional fins or multi-fin arrays are often used. Effective heat dissipation rates exceeding 1.0 W cm^{-2} in natural convection, which are comparable to and in some cases superior to forced convection, can be achieved by attaching a series of sub-fins to the main-fin surface [1, 2] as shown in the configuration of Fig. 1. With an increase in fin dimensions or surface heat fluxes, however, fin efficiencies decrease significantly, as well as incurring problems with weight, size, etc. Therefore, further improvement in heat dissipation is strongly dependent on the increasing of fin efficiencies, i.e. the reducing of thermal conductive resistance in fins.

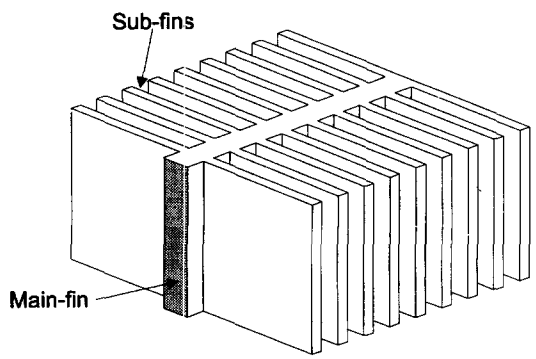

Fig. 1. A multi-fin array configuration.

An effective device for reducing conductive resistance is the heat pipe, which serves as a highly conductive path between the heat source and sink. In recent years, planar heat pipes have been proposed to replace conventional heat sinks used in space and electronics applications [3, 4], owing to their high conductivity and reduced weight. The heat dissipation often corresponds to an electronic chip attached directly to the surface of a planar heat pipe with the rest of the pipe simply exposed to the ambient. Ogushi *et al.* [5, 6] investigated the fundamental characteristics of a grooved planar heat pipe for space applications because of its lighter weight and smaller temperature difference between the evaporator and condenser. Peck and Fleischman [7] designed a light-weight aluminum heat pipe panel for use as an efficient space radiator. Um and Chow [8] examined temperature distribution and gravity effect on the heat transport capacity of a planar heat pipe. North and Avedisian [9] proposed two heat pipe designs where steady heat fluxes of up to 47 W cm^{-2}, corresponding to a total power dissipation of up to 900 W, were reported for the forced convection module with surface temperatures under 100°C.

In the present study, a novel planar heat pipe, combining a convective fin with phase-change advantage of a heat pipe, is proposed for heat dissipation from high-power equipment. An experimental and analytical investigation was conducted to evaluate the thermal characteristics of the heat pipe in both natural and forced air convection configurations; the latter

† Author to whom correspondence should be addressed.

NOMENCLATURE

A	surface area [m^2]
c_p	specific heat [J kg^{-1} K^{-1}]
g	acceleration due to gravity [m s^{-2}]
Gr	Grashof number
h	heat transfer coefficient [W m^{-2} K^{-1}]
H	height of the planar heat pipe [m]
H_p	heating height on heat pipe side-wall in localized heating module [m]
i_{lg}	latent heat of vaporization [J kg^{-1}]
L	length of the planar heat pipe [m]
Nu	Nusselt number
Pr	Prandtl number
q	heat flux [W m^{-2}]
Q	total heat input [W]
Ra	Rayleigh number
T	temperature [K]
ΔT	surface temperature drop from the base to the tip [K]
ΔT_w	wall superheat [K]
ΔT_{ONB}	wall superheat necessary to cause nucleation [K]
x, y, z	coordinates in the fin thickness, height and length direction [m].

Greek symbols

β	coefficient of expansion [K^{-1}]
δ	wall thickness of the planar heat pipe [m]
ρ	density [kg m^{-3}]
μ	viscosity [N s m^{-2}]
λ	thermal conductivity [W $m^{-1}K^{-1}$]
λ_{eff}	effective thermal conductivity of the heat pipe [W m^{-1} K^{-1}]
ν	kinematics viscosity [m^2 s^{-1}]
η	fin efficiency.

Subscripts

b	boiling
c	condensation
l	liquid
n	natural convection with evaporation
s	saturated
v	vapor
w	wall
ν	phase-change heat transfer
∞	surroundings.

was attempted to simulate the enhanced natural heat rejection of mounting a sub-fin array on the condenser. The current research is unique in several aspects. While heat pipes have been extensively examined in previous investigations, none have considered the performance of planar heat pipes used directly as convective fins or in multi-fin arrays, which are lighter and much more efficient than conventional solid metal fins or fin arrays. Also, separated evaporator and condenser sections, as well as virtually no adiabatic section (Fig. 2) are used. This is done to improve the heat dissipation by reducing the flow resistance of vapor and condensate, where two-phase flow patterns as well as heat transfer characteristics are different from that of conventional heat pipes. Additionally, both natural and forced convection configurations are considered and the heat pipe is mounted vertically, which allows gravity to enhance the heat pipe performance.

EXPERIMENTAL DESCRIPTION

As shown the schematic and coordinate system in Fig. 2, the heat pipe was mechanically machined from a 100 mm × 100 mm rectangle brass plate with a thickness of 5 mm. The recessed volume is divided into evaporating and condensing sections. The evaporating section has a vapor space 1 mm thick, 25 mm wide and 84 mm in height, with a 3.5 mm wall thickness. The vapor space of the condensing section is 3.5 mm thick, 50 mm wide, and 84 mm in height, with a 1 mm wall thickness. Both sections have miniature triangular grooves on the inner surfaces with a depth of 0.5 mm and a spacing of 1 mm. The heat pipe is charged with approximately 6 g of pure water as the working fluid. This value is sufficient to cover the evaporating surface with bubbles and liquid film in most tests. Condensate is returned by gravity. A Plexiglas cover with a thickness of 15 mm is attached to the front of the brass body for observations of bubbles and liquid flow. A copper block containing a cartridge heater is used as a heating source, which is soldered to the side wall of the heat pipe and covered with Teflon and styrene foam for insulation.

The heat flux into the heat pipe was determined by measuring temperature gradients at the base of the heat pipe, where three thermocouples were soldered horizontally in-line (in the y-direction) with 4 mm between them. The power added with the heater was also obtained by measuring the voltage and the current with two multimeters. The measured input power was about 12% larger than that measured from the temperature gradients. Surface temperatures were measured with 25 copper–constantan thermocouples spot-soldered on the surface of the heat pipe. Another thermocouple was inserted into the inner-bottom of the heat pipe for measuring the liquid temperature. All temperatures were monitored using a data acquisition system. The heat pipe was cooled by either natural or forced convection at an ambient temperature of about 23°C. In the forced convection configuration, air was blown over the heat pipe by a fan, and the air velocity was measured by a hot-line anemometer. In the

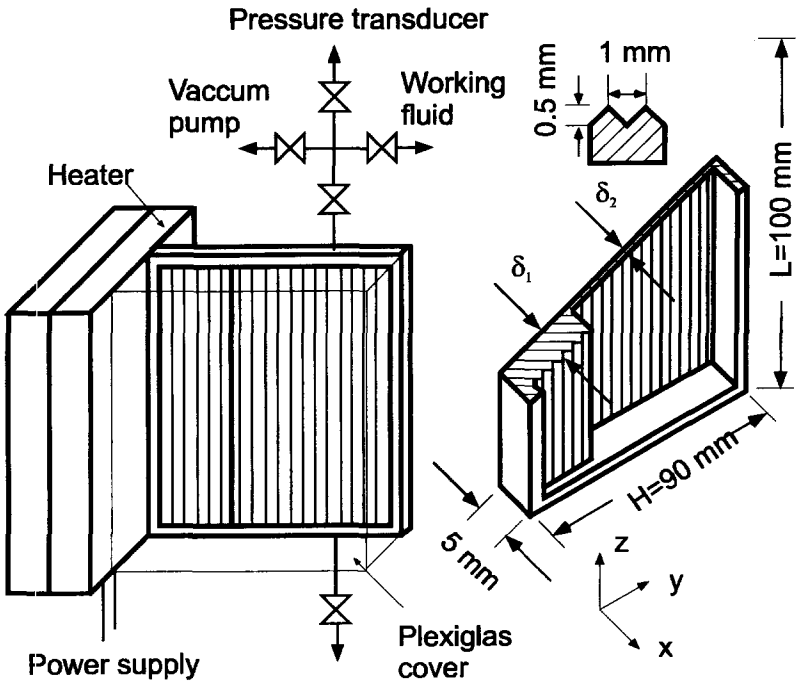

Fig. 2. Schematic and coordinate system of the planar heat pipe.

present study, an average air velocity of 3.8 m s^{-1} was measured by averaging velocities measured at four locations in the upwind cross sectional area of the heat pipe.

Experimental tests were performed in two heated configurations. One was the fully heated module where the entire side-wall area of the heat pipe was exposed to the heat flux. The second was a localized heated module where only the lower quarter of the side-wall area of the heat pipe was exposed to the heat flux (Figs. 7, 8), approximating the thermal performance of a large planar heat pipe, i.e. having a large cooling area to heating area ratio.

As a comparison, experimental tests were also run on the heat pipe with no working fluid. The enhancement of thermal efficiency was found by comparing the performance of the heat pipe, the uncharged heat pipe and a solid brass fin with the same dimensions.

Experimental tests were conducted at a series of different input heat fluxes, while taking care to ensure the base temperature of the heat pipe was never allowed to exceed 120°C. Data were taken at a steady-state condition, which was achieved when the base temperatures of the heat pipe did not vary by more than 0.2°C over a twenty minute period. The temperature measurement error was estimated to be 0.5°C. The heat loss from the heater to the surroundings was roughly 12% of the electrical power input. The uncertainty in the measured air velocity was estimated to be a maximum of 15%.

THEORETICAL FORMULATION

In addition to the experimental measurement, the parameter effects on the thermal characteristics of the heat pipe are analyzed on the basis of a simple model. The following assumptions are employed. Firstly, the vapor and liquid within the heat pipe are assumed to have a uniform saturated temperature and a constant pressure by neglecting pressure drops in their flows. Secondly, different heat transfer mechanisms are assumed on the inner surface exposed to the vapor, i.e. natural convection with evaporation, saturated nucleate boiling and condensation. Finally, temperature gradients in the wall (in the x-direction) are neglected, since the dimension of pipe wall thickness is much smaller than that of pipe height and length. Additional assumptions include homogeneous, isotropic and constant thermal properties.

The energy governing equation is

$$\lambda_w \delta\left(\frac{\partial^2 T}{\partial y^2}+\frac{\partial^2 T}{\partial z^2}\right)=h_\infty(T-T_\infty)+h_v(T-T_s) \quad (1)$$

where the phase-change heat transfer coefficient h_v has different forms depending on the local wall temperature T_w or the wall superheat ΔT_w [10]. For natural convection with evaporation ($\Delta T_w \leqslant \Delta T_{ONB}$):

$$Nu = C_2(v_\infty/v_w)^{0.17} Ra^{*1/5} \quad 10^5 \leqslant Ra^* \leqslant 3\times 10^{13} \quad (2)$$

$$C_2=\left(\frac{Pr}{4+9\sqrt{Pr}+10Pr}\right)^{1/5} \quad (3)$$

$$Ra^* = Gr^* Pr = Gr\ Nu\ Pr \quad (4)$$

$$Gr = g\beta(T_w - T_l)z^3/\nu_l^2. \quad (5)$$

For nucleate boiling ($\Delta T_w > \Delta T_{ONB}$):

$$Nu = 0.246 \times 10^7 X_1^{0.673} X_3^{1.26} X_4^{-1.58} X_{13}^{5.22} \quad (6)$$

$$10^{-4} \leqslant p/p_c \leqslant 0.886 \quad \beta = 45°$$

$$Nu = hd/\lambda_l \quad d = 0.0146\beta(2\sigma/g(\rho_l - \rho_v))^{1/2} \quad (7)$$

$$X_1 = qd/(\lambda_l T_s) \quad X_3 = c_{pl} T_s d^2/a_l^2,$$

$$X_4 = i_{lg} d^2/a_l^2, \quad X_{13} = (\rho_l - \rho_v)/\rho_l.$$

For film condensation ($T_w < T_s$):

$$h = 0.943\left(\frac{g\rho_l(\rho_l - \rho_v)\lambda_l^3(i_{lg} + 0.68c_{pl}\Delta T_w)}{L\mu_l(T_s - T_w)}\right)^{1/4}. \quad (8)$$

The boundary conditions are

$$\lambda_w \frac{\partial T}{\partial z} = -h_\infty(T - T_\infty) \quad z = 0 \quad \text{and} \quad z = L \quad (9)$$

$$\lambda_w \frac{\partial T}{\partial y} = -h_\infty(T - T_\infty) \quad y = H \quad (10)$$

$$-\lambda_w \frac{\partial T}{\partial y} = \dot{q} = \text{const.} \quad y = 0$$

for constant input heat flux (11)

$$T = \text{const.} \quad y = 0$$

for constant base temperature. (12)

Considering an overall thermal balance of the working fluid, the convection and evaporating heat transfer should be equal to the condensing heat transfer, i.e.

$$\int_{A_b}\int h_b(T)(T - T_s)dA_b + \int_{A_n}\int h_n(T)(T - T_s)dA_n + \int_{A_c}\int h_c(T)(T - T_s)dA_c = 0. \quad (13)$$

Equations (1)–(13) were solved numerically by a finite difference procedure using an iteration approach. Calculations were carried out under a variety of conditions, including constant input heat flux, constant base temperature, various pipe dimensions, fully and localized heating configurations, in natural and forced convection, etc., to investigate the influence of these parameters on the performance of the heat pipe, compared with that of the uncharged heat pipe and solid metal fin.

RESULTS AND DISCUSSION

From the experiments, the heat transfer characteristics of the planar heat pipe are found to depend strongly on the boiling behavior within the narrow evaporating section. At lower input heat fluxes, e.g. $\dot{q} < 0.5$ W cm^{-2} in natural convection, the primary heat transfer mode is natural convection with evaporation at the liquid–vapor interface, as no bubbles were observed. With increasing heat fluxes, especially for the forced convection, boiling occurred with bubbles that formed and coalesced on the lower portion of the heating surface. At high input heat fluxes, e.g. $\dot{q} > 5$ W cm^{-2} for forced convection, elongated bubbles were periodically formed and a thin liquid film was observed on the heating surface. The boiling heat transfer is thought to be enhanced by the forced removal of superheated liquid and the evaporation of the thin film. Increasing the heat flux still further, however, resulted in slugging liquid flushed from the evaporating section into the upper portion of the condensing section and a liquid-deficient region formed on the heating surface, both of which degraded the thermal performance of the heat pipe.

The performance of the heat pipe is determined experimentally by surface temperature measurements. Temperature readings from five thermocouples mounted vertically along the pipe length (in the z-direction) are averaged to produce a temperature distribution along the pipe height (in the y-direction). Typical temperature distributions for natural and forced convection are shown in Figs. 3 and 4, respectively. Measurements are presented for the water-charged and the uncharged heat pipe, and the performance of a solid brass fin with the same dimensions is also

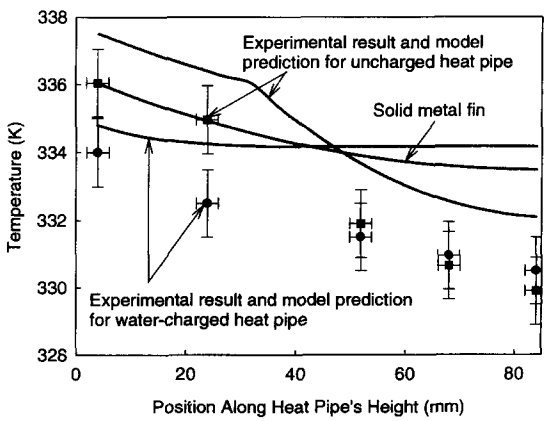

Fig. 3. Surface temperature distributions in natural convection ($\dot{q} = 0.8 \pm 0.15$ W cm^{-2}).

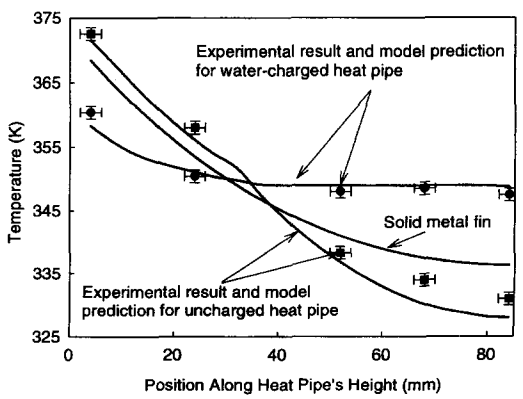

Fig. 4. Surface temperature distributions in forced convection ($\dot{q} = 9.6 \pm 1.5$ W cm^{-2}).

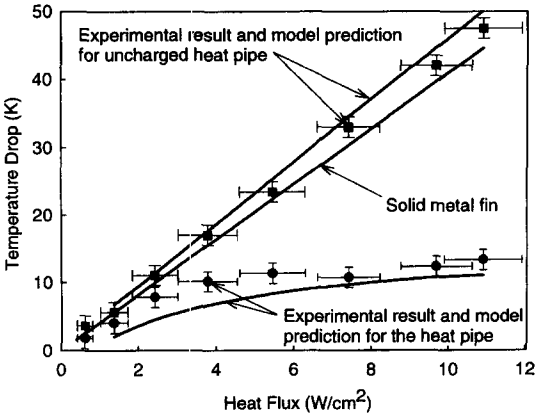

Fig. 5. Surface temperature drop versus input heat flux.

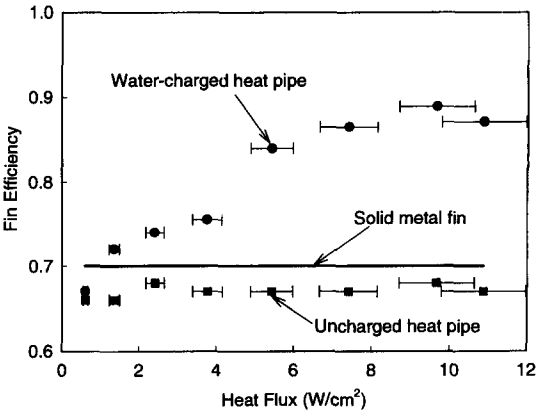

Fig. 6. Enhancement of fin efficiency by the planar heat pipe.

illustrated for reference. In Fig. 3, for a low input heat flux in natural convection, no major difference is observed between the charged and the uncharged heat pipe. The majority of the input is conducted through the pipe wall rather than being removed through phase change of the working fluid. In Fig. 4, however, significant differences are observed for a high input heat flux during forced convection. The heat pipe shows a much more uniform temperature distribution and a much lower heating temperature than the uncharged pipe and the solid fin. The temperature drop (from the base to the tip) is significantly decreased, yielding 13, 34 and 42°C for the heat pipe, solid fin and uncharged heat pipe, respectively.

Variations of the temperature drop with input heat flux during forced convection are shown in Fig. 5. At low heat fluxes, the temperature drop increases with heat flux increases with nearly the same trend for all three configurations. However, with increasing the heat flux, the increasing rate of the temperature drop with heat flux decreases rapidly, as is expected with effective boiling and condensing heat transfer. The thermal resistance of the heat pipe is found to be more than three times smaller than that produced by the solid fin when the heat flux is over 10 W cm^{-2}. Also note that the effective conductivity of the heat pipe, which can be expressed simply as $\lambda_{\text{eff}} \propto \dot{q}W/\Delta T$, is strongly dependent on the input heat flux and the pipe height.

The enhancement of thermal efficiency is shown in Fig. 6. The fin efficiency is defined as the ratio of actual heat dissipated by the fin (or the heat pipe) to the ideal heat dissipated if the entire fin is operating at a temperature difference existing at the fin base (or the pipe base). Roughly a 22% increase in fin efficiency is obtained by the heat pipe when compared with a solid brass fin with the same dimensions. Unlike solid fins, the efficiency of the heat pipe is also affected by the heat input since it strongly depends on the boiling and condensing heat transfer, as mentioned above.

As an approximate approach, experiments were also performed in a localized heated module to simulate performance of the heat pipe having a large ratio of cooling area to heating area. Surface temperature contours of the charged and the uncharged heat pipe, based on the experimental measurements for natural and forced convection, are shown in Figs. 7 and 8, respectively. In both convection cases, the heat pipe shows much more uniform temperature distributions and lower heating temperatures than the uncharged pipe. The experimental results indirectly demonstrate that a high thermal efficiency can be maintained by the planar heat pipe even for a large pipe dimension. Furthermore, dimensional influences on the thermal performance are compared between a planar heat pipe and a solid brass fin. The analysis is performed for heat pipes having a length to height ratio of 10 : 9 and a thickness of 5 mm, a constant base temperature of 373 K, and a convection coefficient of 35 W m^{-2} K^{-1}. In Fig. 9, a significant enhancement in the heat dissipation rate, as well as a high thermal efficiency, is achieved by the heat pipe compared with a solid fin having the same dimensions. The effective conductivity of the heat pipe is strongly dependent on the pipe height, so that for large pipe heights, the advantage of using the heat pipe as a high-conductivity path becomes more pronounced.

Another important effect on the performance of a planar heat pipe is the surface air convection. In natural convection, as shown the experiment above, the advantage of using a planar heat pipe may not be significant, where the convective resistance hinders the effect of the heat pipe yield. When coupled with forced convection, or area enhancement by attaching a fin array on the condenser region (since forced convection is often precluded in applications due to reliability concerns), however, much higher heat dissipation rate can be derived, where the heat pipe forms a high thermal conductivity path between the heating surface and sub-fins. An analysis of convection influences on the heat pipe performance is illustrated in Fig. 10, where the heat pipe as well as the solid fin, has the same configuration as the one used in the experiments. With increasing air convection

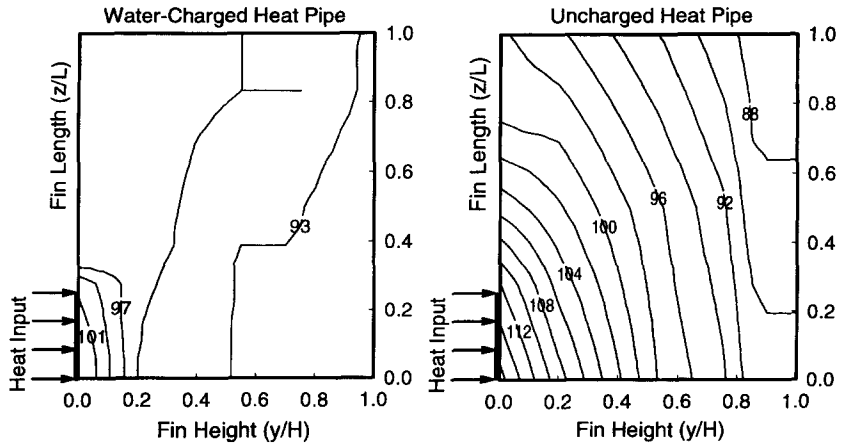

Fig. 7. Surface temperature contours in the localized heating module ($\dot{q} = 12.1 \pm 2.0$ W cm^{-2} in natural convection).

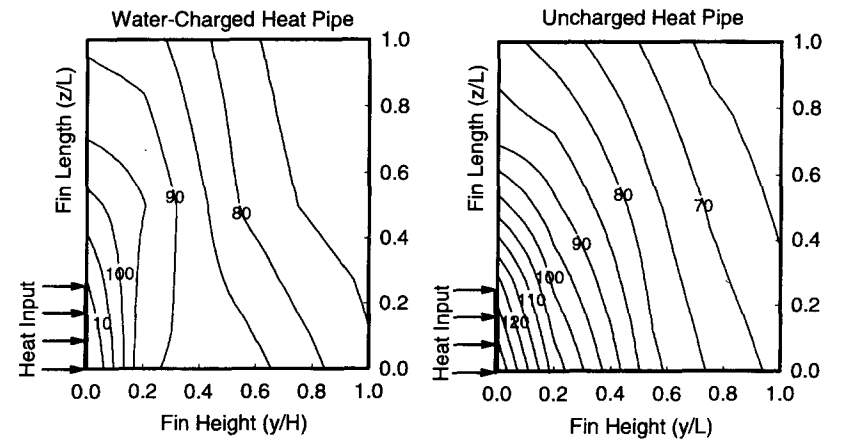

Fig. 8. Surface temperature contours in the localized heating module ($\dot{q} = 33.7 \pm 5.0$ W cm^{-2} in forced convection).

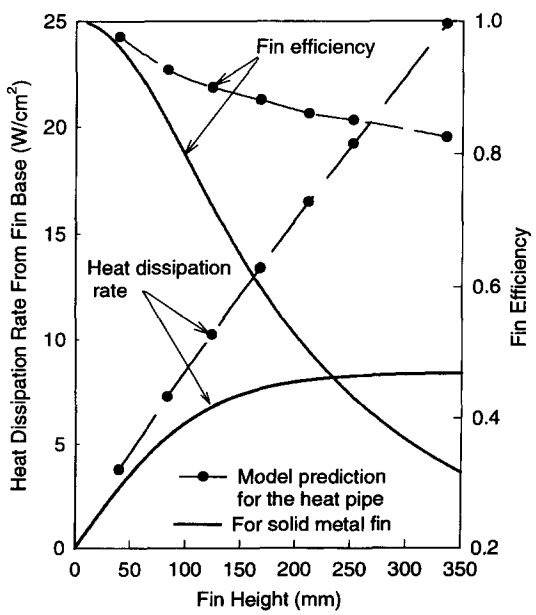

Fig. 9. Influences of heat pipe dimensions ($T_b = 373$K, $h_\infty = 35$ W m^{-2} K^{-1}).

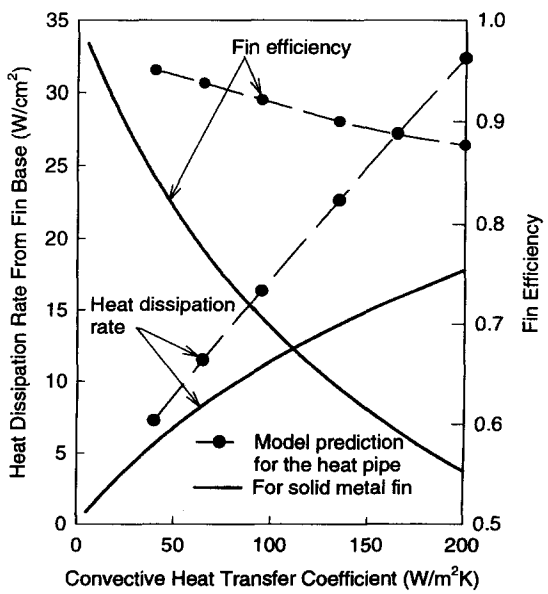

Fig. 10. Influences of convection coefficients ($T_b = 373$K).

coefficients, the heat pipe shows a much higher heat dissipating ability and thermal efficiency than the solid fin. While for a solid fin, increasing air convection seriously impedes the efficiency due to the inherent conductive resistance.

CONCLUDING REMARKS

A novel planar heat pipe has been developed and evaluated both experimentally and analytically. A wide range of heat input configurations is examined experimentally by considering boiling heat transfer characteristics, temperature distributions and thermal efficiencies. Furthermore, effects of pipe dimension and surface convection on the heat dissipating capability and thermal efficiency of the heat pipe are discussed in detail.

The heat pipe shows a significant improvement in effective thermal conductivity with nearly uniform temperature distributions and lower heating temperatures, compared with the solid fin. Planar heat pipes do not suffer from a seriously reduced thermal efficiency for large dimensions or in enhanced surface cooling, as classical fins do. Meanwhile, the heat dissipation rate by a planar heat pipe is strongly dependent on the pipe height and the effective surface convection; either improvement will significantly increase the heat dissipation capability of a heat pipe. The results indicate that planar heat pipes are potentially a viable alternative to large bulky metal fin structures used in many industrial applications, particularly those requiring both high-density heat dissipation and high system reliability.

Acknowledgements—The authors gratefully acknowledge technical support from HITACHI Ltd, and would like to thank Dr Jon P. Longtin for insightful discussions and comments on the work.

REFERENCES

1. Hanneman, R., Thermal control for mini and microcomputers: the limits of air cooling. *Bulletin of the International Centre for Heat & Mass Transactions*, 1989, **3,** 65–83.
2. Bar-Cohen, A. and Jelinek, M., Optimum arrays of longitudinal rectangular fins in convective heat transfer. *Heat Transfer Engineering*, 1985, **6,** 68–77.
3. Vafai, K. and Wang, W., Analysis of flow and heat transfer characteristics of an asymmetrical flat plate heat pipe. *International Journal of Heat & Mass Transfer*, 1992, **35,** 2087–2099.
4. McCreery, G. E., A two-dimensional "flat" heat pipe for the study of liquid flow and vapor formation phenomena. *ASME Topics in Heat Transfer*, 1992, **HTD-206-3,** 83–88.
5. Ogushi, T., Murakani, M., Masumoto H. and Hayashi, R., Study in newly developed flat plate heat pipe heat sink. *National Heat Transfer Conference*, 1988, Vol. 1 pp. 517–521.
6. Ogushi, T., Murakami, M., Takada, T., Yao, A., Sakurai, Y. and Masumoto, H., Experimental investigation of a flat plate heat pipe and cold plates in thermal management system under micro-gravity environment. AIAA-91-1360, 1991.
7. Peck, S. J. and Fleischman, G. L., Lightweight heat pipe panels for space radiators. *Proceedings of Sixth International Heat Pipe Conference*, 1987, pp. 262–267.
8. Um, J., Chow. L. C. and Baker, K., An experimental investigation of flat plate heat pipe. *ASME Fundamentals of Heat Pipes*, 1994, **HTD-278,** 21–26.
9. North, M. T. and Avedisian, C. T., Heat pipes for cooling high flux/high power semiconductor chips. *Journal of Heat Transfer*, 1993, **115,** 112–117.
10. Heat Transfer, *JSME Data Book*, 4th edn, Chaps. 2, 4, 5. JSME Press, Tokyo, 1987.